Supporting Information

Albertazzi et al. 10.1073/pnas.1303109110

SI Text

SI Methods

Chemicals were purchased from Sigma-Aldrich and used without further purifications. Cy3-*N*-hydroxy succimide (NHS) and Cy5-NHS esters were purchased from Lumiprobe. DNA oligos with different length were obtained from Eurofins. Dialysis membranes were obtained from Spectrum Laboratories. Flash chromatography was performed on a Biotage flash chromatography system using 200–425 mesh silica gel (type 60A, grade 633). Water was purified on an EMD Millipore Mili-Q Integral Water Purification System. ^{1}H-NMR and ^{13}C-NMR spectra were recorded on a Varian Mercury Vx 400 MHz (100 MHz for ^{13}C) or a Varian Mercury Plus 200 MHz (50 MHz for ^{13}C) NMR spectrometer. Chemical shifts are given in parts per million (δ) values relative to residual solvent or tetramethylsilane (TMS). Splitting patterns are labeled as s, singlet; d, doublet; dd, double doublet; t, triplet; q, quartet; quin, quintet; m, multiplet; and b stands for broad. Matrix-assisted laser desorption/ionization mass spectra were obtained on a PerSeptive Biosystems Voyager DE-PRO spectrometer or a Bruker autoflex speed spectrometer using α-cyano-4-hydroxycinnamic acid (CHCA) and 2-[(2*E*)-3-(4-*tert*-butylphenyl)-2-methylprop-2-enylidene]malononitrile (DCTB) as matrices. Infrared spectra were recorded on a Perkin-Elmer Spectrum One 1600 FT-IR spectrometer or a Perkin-Elmer Spectrum Two FT-IR spectrometer, equipped with a Perkin-Elmer Universal ATR Sampler Accessory.

Synthetic Procedures

The synthetic scheme for the synthesis of cationic BTA^{3+} is reported in Fig. S1. The detailed procedures for the synthesis are reported in the following. The synthesis of neutral pegylated 1,3,5-benzenetricarboxamide derivatives (BTAs) was previously reported (1).

Tetraethylene glycol monotosylate (1). A round-bottom flask (1 L) was charged with tetraethylene glycol (0.51 mol, 99.4 g) and THF (100 mL). The mixture was placed in an ice bath and NaOH (0.078 mmol, 3.10 g) was dissolved in water (18 mL) and added carefully. The mixture was stirred for 15 min and *p*-toluenesulfonyl chloride (0.052 mmol, 10.0 g), dissolved in THF (200 mL), was added in 2 h using an addition funnel. The mixture was stirred for 2 h. Water (300 mL) was added and the THF was removed in vacuo. The remaining aqueous mixture was extracted three times with dichloromethane (200 mL). The organic fractions were combined and washed three times with water (200 mL). The organic layer was washed with brine (200 mL) and dried with sodium sulfate. The obtained material was purified by dry column vacuum chromatography (column diameter, 6 cm; height, 6 cm) (eluent heptane/ethyl acetate, 100/0–0/100, followed by ethyl acetate/methanol, 90/10) yielding nr. Yield = 12.8 g, 71%. ^{1}H NMR (400 MHz, $CdCl_3$ δ): 7.80 (d, J = 8.3 Hz, 2H, aromatic), 7.34 (d, J = 8.0 Hz, 2H, aromatic), 4.17 (t, J = 4.8 Hz, 2H, CH_2-O-S), 3.82–3.53 [m, 14H, O-$(CH_2)_2$-O], 2.45 (s, 3H, Ar-CH_3).

Azidotetraethylene glycol (2). A round-bottom flask (500 mL) was charged with tetraethylene glycol monotosylate nr (0.031 mmol, 10.83 g) and ethanol was added (200 mL). To the stirring solution, sodium azide (0.091 mmol, 5.93 g) was added. The reaction mixture was heated to reflux and stirred for 22 h. The reaction mixture was diluted with brine (200 mL), and the ethanol was removed in vacuo. The aqueous mixture was extracted two times with chloroform (200 mL). The organic fractions were combined, washed with brine (100 mL), and dried with sodium sulfate. The obtained material was dissolved in acetonitrile (100 mL), concentrated in vacuo, and this was repeated with toluene (100 mL). Yield = 6.7 g, 98%. ^{1}H NMR (400 MHz, $CdCl_3$ δ): 3.81–3.57 [m, 14H, O-(CH_2))], 3.40 (t, J = 4.9 Hz, 2H, N3-CH_2), 2.49 (t, J = 6.0 Hz, 1H, CH_2-OH). ^{13}C NMR (100 MHz, $CdCl_3$ δ): 72.47, 70.72, 70.69, 70.62, 70.37, 70.06, 61.78, 50.68.

Azidotetraethylene glycol-12-bromododecyl ether (3). A round-bottom flask (250 mL) was charged with azidotetraethylene glycol (**2**) (38.8 mmol, 8.5 g), and THF (160 mL) was added. The stirred solution was placed in an ice bath and sodium hydride (60% in mineral oil, 2.1 g, 52.5 mmol) was added in portions. After 1 h, the ice bath was removed and 1,12-dibromododecane (0.26 mol, 87 g) was added. The mixture was stirred at room temperature overnight. The mixture was filtered, and the filtrate was concentrated in vacuo. The obtained material was dissolved in hot methanol. Upon cooling, a large portion of the 1,12-dibromododecane crystallized out and was removed by filtration. The filtrate was concentrated, yielding an oil that was purified by dry column vacuum chromatography (column diameter, 6 cm; height, 6 cm) (eluent heptane/ethyl acetate, 100/0–50/50). Yield = 7.4 g, 41%. ^{1}H NMR (400 MHz, $CdCl_3$ δ): 3.76–3.53 [m, 14H, O-$(CH_2)_2$-O], 3.51–3.33 (m, 6H, $CH_2CH_2CH_2O$, CH_2CH_2Br, N_3-CH_2), 1.93–1.79 (m, 2H, CH_2CH_2Br), 1.62–1.51 (m, 2H, $CH_2CH_2CH_2O$), 1.47–1.37 (m, 2H, $CH_2CH_2CH_2O$), 1.37–1.16 (m, 14H, aliphatic). ^{13}C NMR (100 MHz, $CdCl_3$ δ): 71.53, 70.70, 70.68, 70.63, 70.62, 70.59, 70.04, 70.02, 50.68, 34.05, 32.82, 29.62, 29.55, 29.52, 29.50, 29.46, 29.41, 28.75, 28.16, 26.07.

Azidotetraethylene glycol-12-phthalimidododecyl ether (4). A round-bottom flask (250 mL) was charged with azidotetraethylene glycol-12-bromododecyl ether (**3**) (13.6 mmol, 6.34 g) and methyl isobutyl ketone (MIBK) (80 mL). To the mixture, 18-crown-6 (1.9 mmol, 0.50 g) and potassium phthalimide (40.5 mmol, 7.5 g) were added, and the mixture was stirred at reflux overnight. The reaction mixture was allowed to cool to room temperature and, subsequently, filtrated. The filtrate was concentrated in vacuo and purified by column chromatography (eluent heptanes/ethylacetate, 100/0–0/100). Yield = 6.4 g, 88%. ^{1}H NMR (400 MHz, $CdCl_3$ δ): 7.84 (dd, J = 5.4, 3.0 Hz, 2H, phthalimide), 7.70 (dd, J = 5.4, 3.1 Hz, 2H, phthalimide), 3.74–3.51 [m, 16H, O-$(CH_2)_2$-O, $CH_2CH_2CH_2N$], 3.44 (t, J = 6.8 Hz, 2H, $CH_2CH_2CH_2O$), 3.38 (t, J = 5 Hz, 2H, N_3-CH_2), 1.74–1.62 (m, 2H, $CH_2CH_2CH_2N$), 1.59–1.46 (m, 2H, $CH_2CH_2CH_2O$), 1.38–1.18 (m, 16H, aliphatic). ^{13}C NMR (100 MHz, $CdCl_3$ δ): 168.46, 133.81, 132.19, 123.13, 71.55, 70.71, 70.69, 70.64, 70.63, 70.61, 70.05, 70.03, 50.69, 38.08, 29.68–29.44, 29.19, 28.60, 26.87, 26.09.

Azidotetraethylene glycol-12-aminododecyl ether (5). A round-bottom flask (250 mL) was charged with azidotetraethylene glycol-12-phthalimidododecyl ether (**4**) (12.0 mmol, 6.4 g) and ethanol (160 mL). To the stirring solution, hydrazine monohydrate (6.0 mL) was added, and the mixture was stirred at reflux overnight. The solvent was removed in vacuo, yielding a white solid. The obtained material was dissolved in dichloromethane (400 mL) and extracted with sodium hydroxide (1 M, 250 mL). The aqueous layer was extracted with dichloromethane (120 mL). The organic fractions were combined, extracted with brine (200 mL), dried with sodium sulfate, filtrated, and concentrated in

vacuo. Yield = 4.7 g, 97%. ^{1}H NMR (400 MHz, $CdCl_3$ δ): 3.76–3.53 [m, 14H, O-$(CH_2)_2$-O], 3.44 (t, J = 6.8 Hz, 2H, $CH_2CH_2CH_2O$), 3.39 (t, J = 4.9 Hz, 2H, N_3-CH_2), 2.68 (t, J = 7.0 Hz, 2H, CH_2CH_2-NH_2), 1.64–1.50 (m, 2H, $CH_2CH_2CH_2O$), 1.49–1.37 (m, 2H, $CH_2CH_2CH_2O$), 1.37–1.12 (m, 16H, aliphatic). ^{13}C NMR (100 MHz, $CdCl_3$ δ): 71.52, 70.68, 70.66, 70.62, 70.61, 70.58, 70.03, 70.01, 50.67, 42.28, 33.88, 29.65–29.45, 26.88, 26.07. FT-IR (ATR) ν (cm-1): 3,378, 2,923, 2,853, 2,100, 1,595, 1,465, 1,349, 1,286, 1,250, 1,109, 1,039, 992, 939, 851, 722, 646, 556, 506. Liquid chromatography-MS (electrospray ionization): Rt = 7.47 min, calculated M_r = 402.32 g/mol, observed m/z = 403.50 [MH+].

***N*^{1},*N*^{3},*N*^{5}-tris(1-azido-3,6,9,12-tetraoxatetracosan-24-yl)benzene-1,3,5-tricarboxamide (6).** A round-bottom flask (250 mL) was charged with azidotetraethylene glycol-12-aminododecyl ether (**5**) (1.0 mmol, 0.438 g) and $CHCl_3$ (10 mL) and kept at 0 °C by means of an ice bath. To this stirring solution, 160 mg (1.5 eq) of triethylamine and 90 mg (0.3 eq) of 1,3,5-benzenetricarbonyl trichloride were added. The resulting solution was stirred at 0 °C for 30 min and at room temperature overnight. The product was purified by column chromatography (eluent $CHCl_3$/methanol, 100/0–90/10). Yield = 335 mg, 82%. ^{1}H NMR (400 MHz, $CDCl_3$ δ): 3.75–3.60 [m, 42H, O-$(CH_2)_2$-O], 3.41 (t, 6H, $CH_2CH_2CH_2O$), 3.36 (t, 6H, N_3-CH_2), 3.42 (t, 6H, CH_2CH_2-NH), 1.62–1.12 (m, 60H, aliphatic), 8.36 (s, 3H, Ar-H), 6.70 (s, 3H, CO-NH).

***N*^{1},*N*^{3},*N*^{5}-tris(1-amino-3,6,9,12-tetraoxatetracosan-24-yl)benzene-1,3,5-tricarboxamide (7).** A round-bottom flask (10 mL) was charged with N^1,N^3,N^5-tris(1-azido-3,6,9,12-tetraoxatetracosan-24-yl)benzene-1,3,5-tricarboxamide (**6**) (180 mg) and methanol (5 mL), and N_2 (g) was led through the stirred solution for 10 min. Subsequently, Pd/C (catalytic amount) was added and a balloon filled with H_2 (g) was connected. The reaction mixture was vigorously stirred under H_2 (g) atmosphere overnight at room temperature. The reaction mixture was filtered over celite and concentrated in vacuo, yielding **7** as a yellow wax. Yield = 144 mg, 85%. ^{1}H NMR (400 MHz, $CdCl_3$ δ): 3.75–3.60 [m, 42H, O-$(CH_2)_2$-O], 3.41 (t, 6H, $CH_2CH_2CH_2O$), 2.84 (t, 6H, NH_2-CH_2), 3.42 (t, 6H, CH_2CH_2-NH), 1.62–1.12 (m, 60H, aliphatic), 8.37 (s, 3H, Ar-H), 6.73 (s, 3H, CO-NH). ^{13}C NMR (100 MHz, $CdCl_3$ δ): 165.80, 135.21, 128.12, 73.30, 71.52, 70.60, 70.58, 70.54, 70.25, 70.02, 41.71, 40.33, 29.56, 29.52, 29.49, 29.44, 29.38, 29.2, 26.94, 26.02. MALDI: calculated M_r = 1,284.98 g/mol, observed m/z = 1286.00 [MH+].

General Procedure for BTA^{3+} Labeling. To perform FRET experiments, cationic BTA were labeled either with Cy3 or Cy5 dyes. The conjugation has been achieved by means of commercially available activated NHS esters of the dyes. Briefly, N^1,N^3,N^5-tris(1-amino-3,6,9,12-tetraoxatetracosan-24-yl)benzene-1,3,5-tricarboxamide (**7**) (5 mg) was dissolved in 1 mL of DMSO and triethylamine (5 eq) and Cy dye (0.8 eq) added. The solution was stirred overnight at room temperature and then diluted with 5 mL of water. Purification was achieved by water dialysis (molecular weight cutoff = 1,000 Da) to remove the unreacted dye. Dye conjugation was verified by means of UV-visible spectroscopy and MALDI mass spectroscopy.

Monte Carlo Simulations

We performed μVT lattice Monte Carlo (MC) simulations, in which DNA chains are inserted and removed from the system to establish equilibrium with a reservoir fixed at a bulk concentration of 8.13×10^{-9} chains per lattice site. As an approximation, DNA chains are represented as beads on a lattice connected through bonds, with each bead representing a DNA base. We use a simple cubic lattice in which bonds are allowed between the edges of each site as well as between diagonals sites, yielding to a total of 26 neighbors per lattice site. If we assume that the length of each lattice site corresponds to ∼0.3 nm, we obtain that the bulk concentration of chains is roughly 500 nM in agreement with experimental conditions.

In addition to DNA chains, the system must contain BTA molecules clustered in columnar arrangements. In the interest of simplicity, we represent only a single one of these columnar clusters, by prealigning BTA molecules (represented as single lattice sites) along the z direction. Because of the periodic boundary conditions, the cluster becomes effectively of infinite length. Because BTA molecules are not allowed to move in the x–y plane but can only exchange position with other (aligned) BTA molecules, the cluster preserves its original shape during the simulation. Also, to this level of approximation, BTA molecules interact with each other only through excluded volume interactions (i.e., two molecules cannot be in the same lattice site at the same time).

There are three types of BTA molecules: neutral (gray), charged (red), and charged (green). Although all of the BTA molecules exhibit excluded volume interactions with the DNA chains, only the charged BTA molecules experience a nearest-neighbor attraction toward DNA chain beads. In particular, when a bead of a chain is in nearest-neighbor contact with a charged BTA molecule, the system gains an interaction energy equal to $-\varepsilon$. In this work, ε was varied between 0 and 10 kT, with k, Boltzmann's constant, and T, the absolute temperature. An interaction energy of ε = 4.50 kT best represented the experimental conditions. Because BTA molecules are stacked along the z direction, in principle each BTA molecule has four nearest-neighbor sites with which to have potential attractive interactions.

However, because the real system has only three charged sites and the Kuhn length of ssDNA is longer than a single base, we expect that the experimental system will not have a tendency to wrap around the columnar cluster. Therefore, to decrease the tendency of the simulated chains to wrap around the BTA molecules, but preserving the symmetry of the lattice, we further assume that each BTA molecule can only interact attractively with two of the possible four nearest-neighbor sites. Furthermore, we assume that these attractive sites oppose each other in the x–y plane and are stacked on top of each other along the z direction. We expect, however, that the precise choice of geometry and number of attractive sites will have little effect on the very general trends observed during these simulations. This is confirmed by the agreement observed between the experiments and the very general analytical model described below.

Simulations were typically performed on systems with a dimension of 20 × 20 × 8,000 lattice sites. The percentage of charged BTA molecules was varied between 0.25% and 8%, and the length of the DNA chains was varied between 1 and 24 beads. Usually, simulations were run for more than 10^9 MC steps, with each step selected from a pool of insertion/deletion, chain rearrangement, or BTA swap moves, performed in the standard way (2).

Analytical Model Adsorption of Multivalent Agents to a Surface with Mobile Recruiters

As explained in ref. 3, when we have a substrate with receptors in contact with a bulk solution of multivalent agents that have κ ligands that bind those receptors, and we assume that we can divide the surface in lattice sites such that when a multivalent agent binds no other agents can bind on the same lattice site and that each agent can only bind to the n_R receptors within its lattice site, we can express the partition function Ξ of the system as follows:

$$Z = [1 + z \times q(\kappa, n_R, \beta f_B)]^{N_{\max}}, \quad \textbf{[S1]}$$

where $\beta = 1/kT$, z is the activity of multivalent agents in solution, $N_{\max}$ is the number of lattice sites on the substrate, and q is the single-site bound-state partition function. The activity z is defined as $z = \exp(\beta\mu)$, with $\beta\mu = \beta\mu^{\text{ex}} + \ln(\rho/\rho_0)$, with ρ the concentration of the multivalent in bulk solution and ρ_0 the standard concentration (usually 1 mol/L). Because $\beta\mu^{\text{ex}}$, the excess chemical potential tends to zero for dilute solutions, z can be approximated as $z = \rho/\rho_0$. Finally, the single-site bound-state partition function q, which is a function of the number of ligands k, the number of receptors in a lattice site n_R, the free energy of binding βf_B, and the geometry of the system, is defined as the ratio of single-particle partition functions in the bound and unbound state, at the reference concentration.

$$q \equiv \frac{Q^{\text{sp-bound}}}{Q^{\text{sp-unbound}}}\Bigg]_{\rho=\rho_0}, \quad \textbf{[S2]}$$

where $Q^{\text{sp-unbound}}$ is the partition function of a single unbound particle in solution at concentration ρ_0 and $Q^{\text{sp-bound}}$ is the partition function of a single bound particle. Because the ratio of partition functions at is equal to the ratio of probabilities of being bound/unbound, we find that at the reference concentration:

$$q = \frac{P^{\text{bound}}}{P^{\text{unbound}}} = \frac{\sum_{\lambda=1}^{\lambda\max} P(\lambda)}{P^{\text{unbound}}}, \quad \textbf{[S3]}$$

where $P(\lambda)$ is the probability of being bound with λ, and $\lambda_{\max}$ is the maximum number of bonds that an agent can form within its lattice site [i.e., $\lambda_{\max} = \min(\kappa, n_R)$].

Once the function q is obtained, the average number of bound particle is easily obtained from the following:

$$\theta(\kappa, n_R, \beta f_B, z) \equiv \frac{N}{N_{\max}} = \frac{1}{N_{\max}} \frac{\partial \ln Z}{\partial \beta\mu} = \frac{z \times q(\kappa, n_R, \beta f_B)}{1 + z \times q(\kappa, n_R, \beta f_B)}. \quad \textbf{[S4]}$$

Now, in this treatment, we have assumed that each lattice site has exactly n_R receptors. However, in many practical applications, the receptors are mobile and can be "recruited" and "clustered" by the multivalent agents. To achieve this, we need a formalism in which the number of receptors on each lattice site is allowed to fluctuate while the total number of receptors on the surface remains fixed. Strictly speaking, for a finite number of lattice sites this can be achieved by summing over all possible permutation of receptor rearrangements among the lattice sites such that the total number of receptors remained fixed. In general, this constrained sum is difficult to accomplish. However, as the surface in consideration becomes larger, the correlation between the number of receptors in two different lattice sites disappears and each lattice site becomes independent, with the rest of the lattice sites acting as a reservoir that keeps the average number of receptors $<n_R>$ constant. In this limit, we can write the grand canonical partition function Ξ in which the number of receptors (as well as the number of bound colloids) is allowed to fluctuate. Thus, we can write the following:

$$\Xi = \sum_{n_R=0}^{\infty} \frac{e^{\beta\mu_R n_R}[1 + z \times q(\kappa, n_R, \beta f_B)]}{n_R!}, \quad \textbf{[S5]}$$

where μ_R, the receptor chemical potential must be adjusted such that the average number of receptors $<n_R>$ matches the desired value. To achieve this, we obtain the average number of receptors from the following:

$$\begin{aligned} <n_R> &= \frac{d \ln \Xi}{d\beta\mu_R} = \frac{\sum_{n_R=0}^{\infty} \frac{n_R e^{\beta\mu_R n_R}[1 + z \times q(\kappa, n_R, \beta f_B)]}{n_R!}}{\Xi} \\ &= \sum_{n_R=0}^{\infty} n_R \times P(n_R), \end{aligned} \quad \textbf{[S6]}$$

where we have defined in the last equality the normalized probability $P(n_R)$ for a lattice site to have n_R receptors as follows:

$$P(n_R) = \frac{e^{\beta\mu_R n_R}[1 + z \times q(\kappa, n_R, \beta f_B)]/n_R!}{\Xi}. \quad \textbf{[S7]}$$

Similarly, the average number of bound colloids can be found from:

$$\begin{aligned} <\theta(\kappa, \mu_R, \beta f_B, z)> \equiv \frac{<N>}{N_{\max}} &= \frac{1}{N_{\max}} \frac{\partial \ln \Xi}{\partial \beta\mu} \\ &= \frac{1}{\Xi} \sum_{n_R=0}^{\infty} \frac{e^{\beta\mu_R n_R}[z \times q(\kappa, n_R, \beta f_B)]}{n_R!} \\ &= \sum_{n_R=0}^{\infty} \theta(\kappa, n_R, \beta f_B) \times P(n_R), \end{aligned} \quad \textbf{[S8]}$$

where we have used the definition of z and Eq. **S4**. The average number of bonds $<\lambda>$ is found from the analogous relation as follows:

$$<\lambda> = -\frac{\partial \ln \Xi}{\partial \beta f_B} = \frac{-1}{\Xi} \sum_{n_R=0}^{\infty} \frac{e^{\beta\mu_R n_R}\left[z \times \frac{dq(\kappa, n_R, \beta f_B)}{d\beta f_B}\right]}{n_R!}. \quad \textbf{[S9]}$$

As discussed in ref. 3, the precise form of q will be particular to the system being studied. However, a useful limit is obtained when we assume that all of the κ ligands are within reach of the n_R receptors within the lattice; in this case, we have the following:

$$q(\kappa, n_R, \beta f_B) = \sum_{\lambda=1}^{\min(\kappa, n_R)} e^{-\beta f_B \times \lambda} \frac{\kappa! n_R!}{(\kappa - \lambda)! \lambda! (n_R - \lambda)!}. \quad \textbf{[S10]}$$

Although this situation corresponds to a somewhat optimistic case, it provides a reasonable basis to understand the multivalent effects.

Now that we have a formalism calculate the number of bound multivalent particles to a substrate in the case of mobile receptors, we can proceed to compare the behavior of the parameter α defined as follows:

$$\alpha \equiv \frac{d \ln <\theta>}{d \ln <n_R>}, \quad \textbf{[S11]}$$

to compare the selectivity of a system where receptors are mobile with the ones in which the receptors are distributed randomly (Poisson process) but are fixed. The derivative in Eq. **S11** must be carried out numerically, and it is important to note that for each value of $<n_R>$ we must find (implicitly) from Eq. **S6** the appropriate value of μ_R. The results are shown in Fig. S6 for a system with $\kappa = 10$, $\beta f_B = 0$, and $z = 10^{-5}$. We observe that the system with mobile receptors exhibits a higher value of a at

the peak indicating a superior sensitivity to the receptor concentration although in a somewhat narrower range of n_R.

Finally, we can compare the probabilities $P(n_R)$ of finding a lattice site with n_R receptors at different values of βf_B while keeping constant $<n_R \geq 1$, z = 1e-5, and $\kappa = 5$ in Fig. S7. Note that because $<n_R>$ is a function of both βf_B and μ_R, we need to adjust the value of μ_R for each βf_B to keep $<n_R>$ constant.

If the βf_B is large and positive, the particles do not bind and the receptors distribute randomly on the surface and $P(n_R)$ approaches a Poisson distribution. As βf_B becomes more negative, the fraction of empty lattices $P(n_R = 0)$ increases while a peak starts to develop around $n_R = 5$ consistent with clustering or recruiting of receptors by the multivalent agents. Notice that this bimodal distribution persists even in the limit of infinitely strong bonds. Interestingly, at these conditions the system is prevented from adsorbing more particles as all of the receptors are already bound. Hence, at these conditions the surface thermodynamically self-limits the number of bound particles even as the binding strength goes to infinity.

To understand under which circumstances we can find "self-limited" adsorption behavior, it is instructive to plot in Fig. S8 the average number of bound particles as a function of the activity z at a strong binding $\beta f_B = -10$ and $\kappa = 5$. In addition, we plot Fig. S9 the distributions $P(n_R)$ for several values of z. It can be seen that, when the bulk is extremely dilute such that z^*q $(n_R = \kappa) << 1$, particles do not bind to the surface and the distribution of receptors is essentially random. As the concentration increases (remember $z = \rho/\rho_0$ to a first approximation), particles start to bind on the surface primordially in sites with $n_R = 5$ as this is the maximum number of bonds our multivalent agents can form. As a consequence, particles start recruiting receptors and a bimodal distribution with a peak around $n_R = 5$ is observed for $P(n_R)$ (Fig. 4*A*). When $z^*q(n_R = \kappa) \sim 1$, a significant number of particles is bound and recruiting is evident. As z keeps increasing, but still $z^*q(n_R \leq n_R >) << 1$, the multivalent agents recruit all of the receptors and no further particles can be absorbed. At these conditions, the system achieves maximum recruiting and the surface "self-limits" the number of adsorbed particles. This behavior continues until $z^*q(n_R \leq n_R >) \sim 1$ when the number of absorbed particles starts to increase again approaching $\theta \rightarrow 1$, by redistributing the surface receptors among the newly adsorbed particles. It is important to note however, that although at large z the state of saturated surface is thermodynamically stable, it is likely that in practice the system will become kinetically trapped as the rearrangement of bonds, requiring the breakage of strong bonds, is expected to be slow.

1. Leenders CMA, et al. (2013) Supramolecular polymerization in water harnessing both hydrophobic effects and hydrogen bond formation. *Chem Commun (Camb)* 49(19): 1963–1965.
2. Frenkel D, Smit B (2001) *Understanding Molecular Simulation: From Algorithms to Applications* (Academic, San Diego), 2nd Ed.
3. Martinez-Veracoechea FJ, Frenkel D (2011) Designing super selectivity in multivalent nano-particle binding. *Proc Natl Acad Sci USA* 108(27):10963–10968.

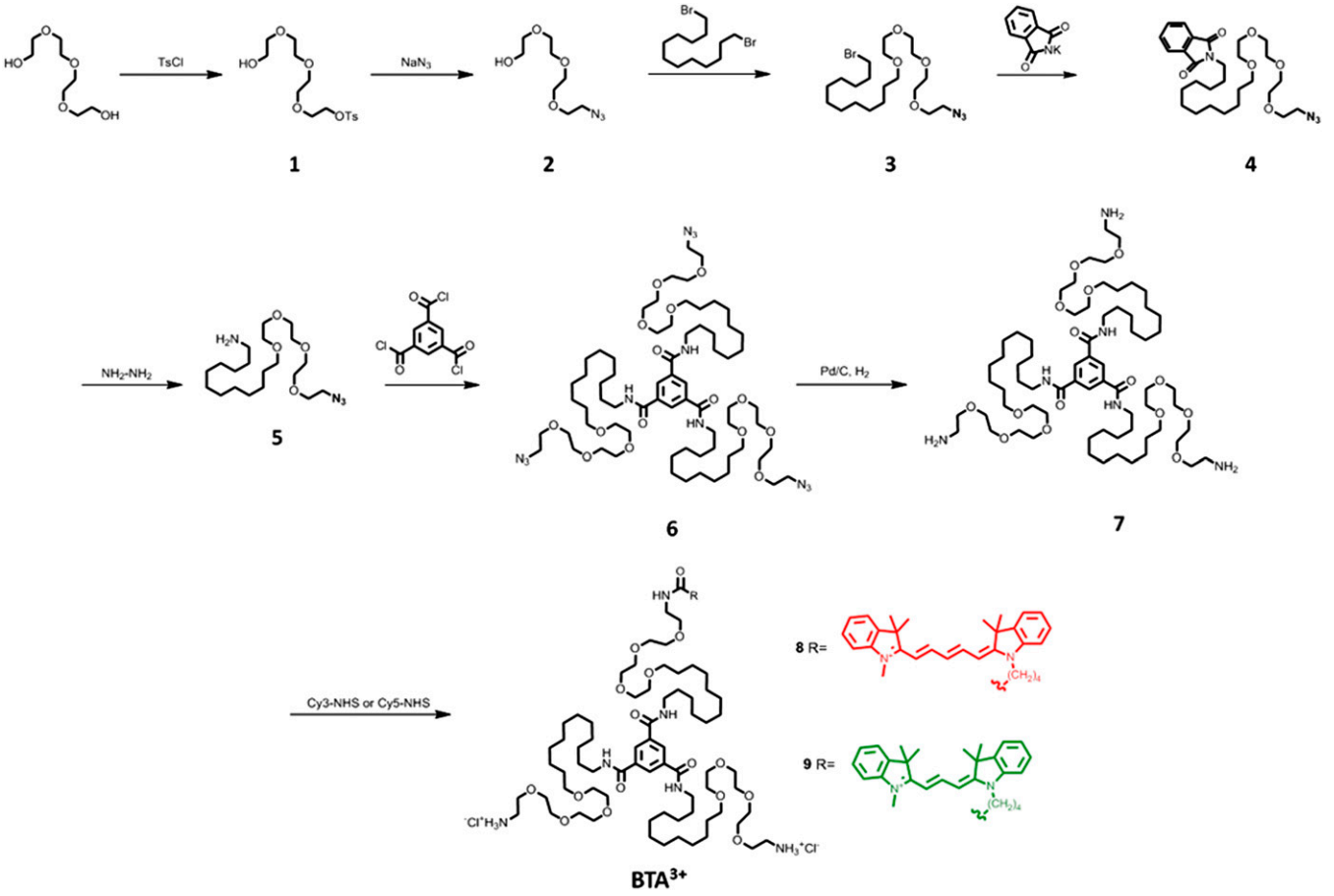

Fig. S1. Synthetic route for cationic BTA^{3+}.

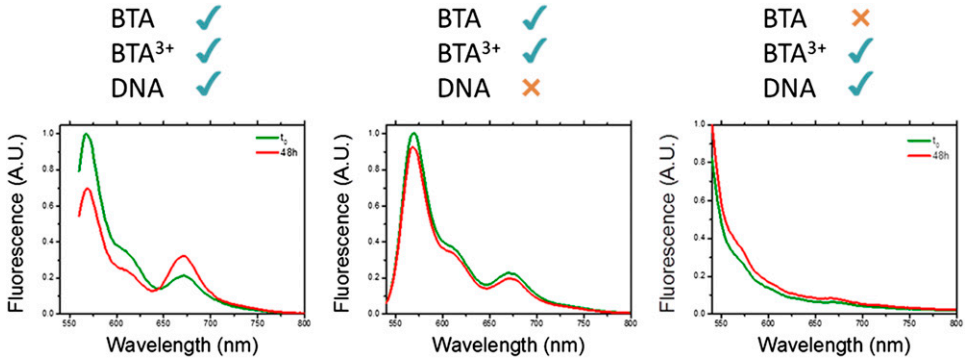

Fig. S2. Emission spectra of DNA-induced clustering. Emission spectra (excitation, 530 nm) of BTA+BTA^{3+} assemblies before (green line) and after (red line) addition of DNA (or water, in the center graph). *Center* and *Right* show no significant changes in the spectra in absence of ssDNA or neutral BTAs, indicating that all of the component are necessary for the noncovalent synthesis of segmented supramolecular polymers. Scattering is observed in the case of the absence of BTA (*Right*) indicating that labeled BTA^{3+} are poorly soluble when not associated to a BTA polymer.

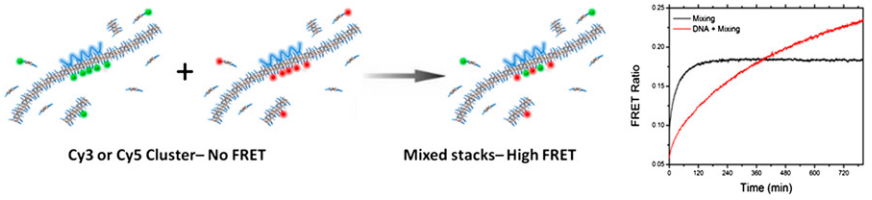

Fig. S3. Dynamic exchange between BTA^{3+} clusters. Schematic representation of the experiment (*Left*). DNA was added to assemblies incorporating either BTA-Cy3 or BTA-Cy5 inducing clustering. After equilibration for 48 h, the two solutions were mixed, measuring the exchange of monomers between clusters. FRET kinetics (*Right*) is slower in the presence of ssDNA, probably due to a slower exchange kinetics due to the DNA/BTA interaction.

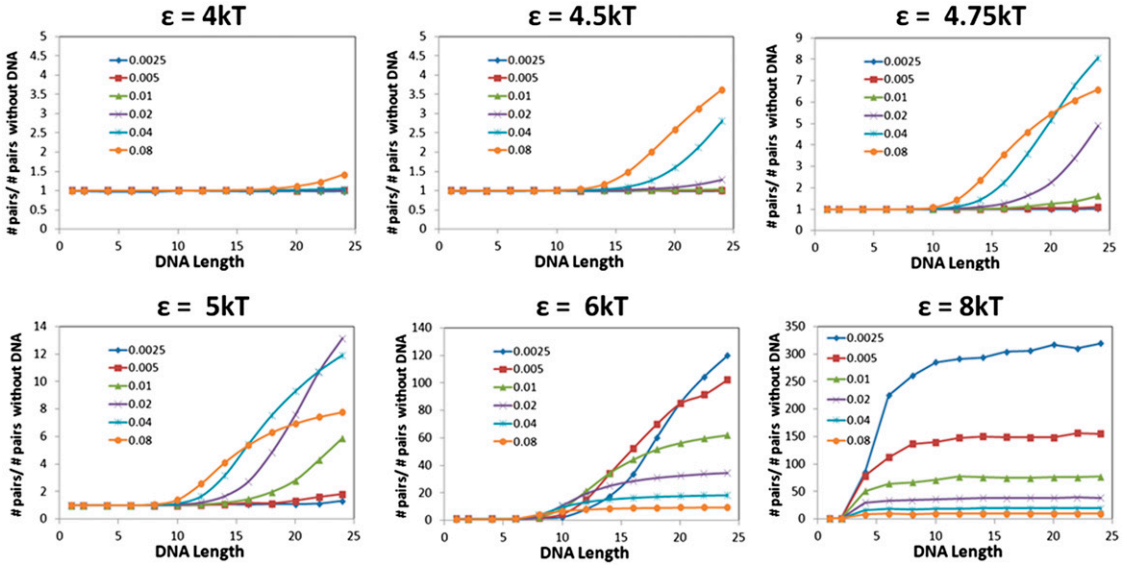

Fig. S4. Normalized number of green–red nearest-neighbor pairs in the μVT MC simulations as a function of the attractive energy ε. For weak binding (ε = 4 kT), DNA chains fail to bind the polymer, and little signal is observed. For the moderate binding (ε = 4.5 kT), the behavior of the signal is similar to the one observed in experiments. However, when ε is further increased, we start to observe "saturation" in which the normalized signal for high receptor concentrations and long DNA chains becomes smaller than at low receptor concentration (ε = 4.75–6 kT). Note, however, that not such saturation exists if we consider the absolute (i.e., nonnormalized) number of green–red pairs as these necessarily always increase with charge concentration. Finally, at very strong binding (ε = 8 kT), all of the normalized curves are saturated and we observed a reversed behavior where little concentration charge has more signal than more concentration charge.

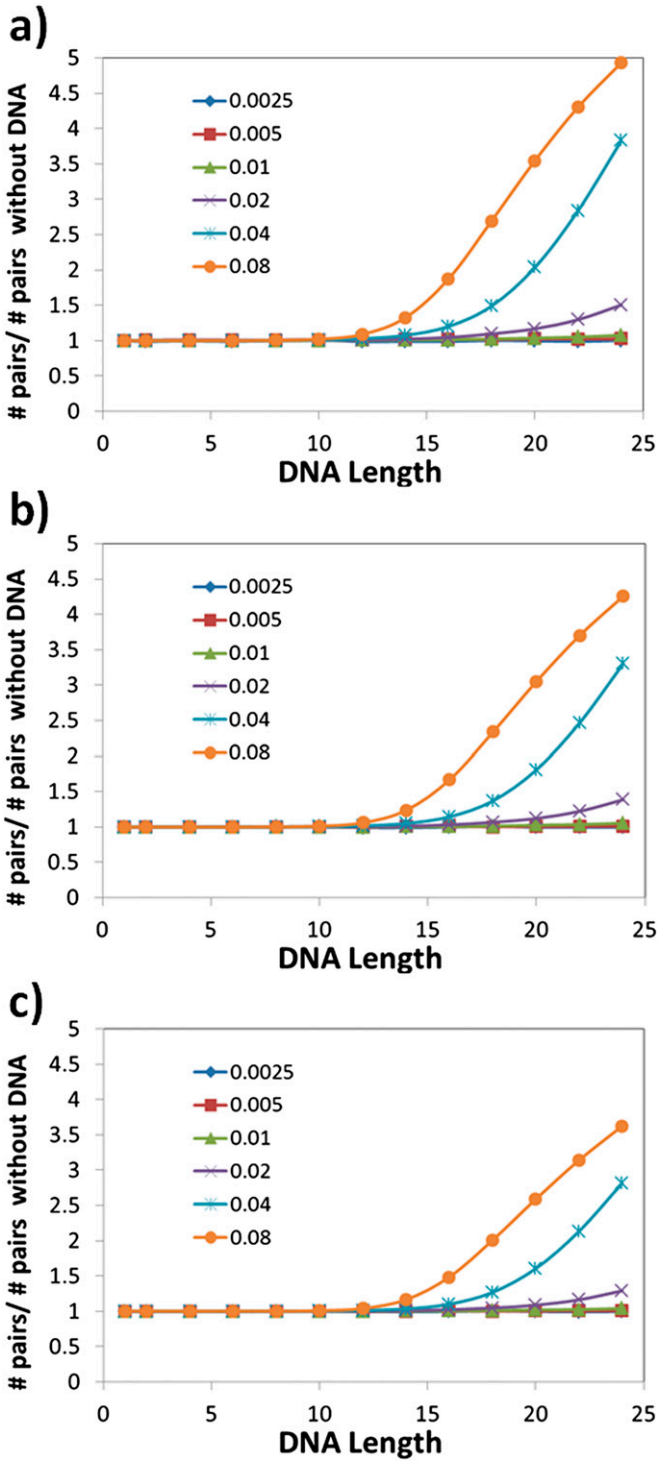

Fig. S5. Average fraction of red–green neighbors as a function of the DNA length. The qualitative behavior of the signal is independent of the number of neighbors considered. (*A*) Only nearest neighbors are considered. (*B*) Up to three neighbors are considered. (*C*) Up to five neighbors are considered.

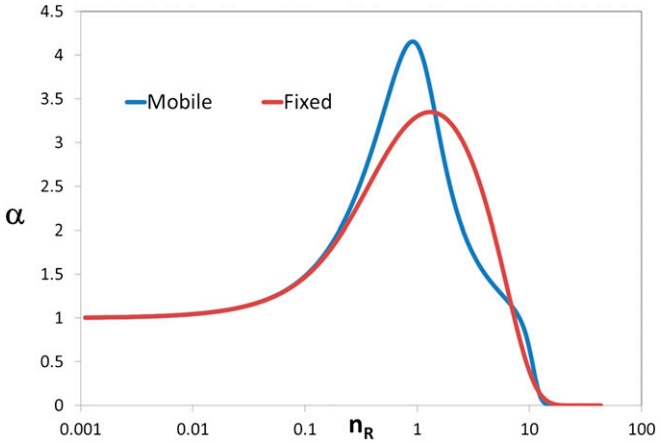

Fig. S6. The value of α as a function of the receptor concentration n_R, in the case of fixed and mobile receptors. The parameters used are $\kappa = 10$, $\beta f_B = 0$, and $z = 10^{-5}$. The mobile receptor system presents a more pronounced peak in α, indicating a sharper dependency to receptor concentration albeit in a narrower range of n_R.

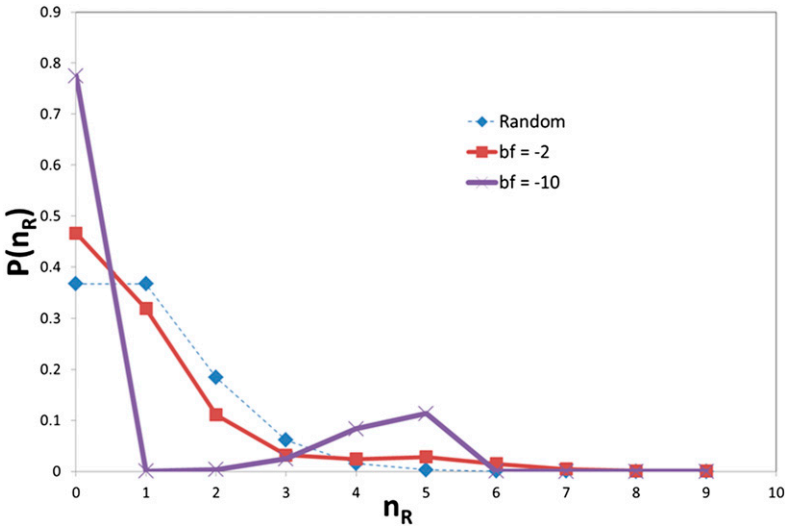

Fig. S7. Probability distributions of finding a lattice site with n_R receptors, for a multivalent system with $<n_R \geq 1$, z = 1e-5, and $\kappa = 5$. As the bond strength increases, the probability distributions deviate from random and become more bimodal, while preserving the mean receptor concentration.

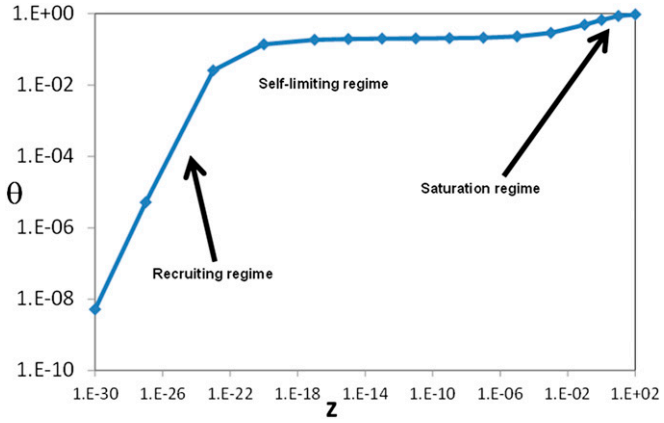

Fig. S8. Fraction of bound particles as function of the activity z at strong binding $\beta f_B = -10$ and $\kappa = 5$. When the bulk concentration is extremely low (i.e., low z), the number of bound particles increases linearly with z. At these conditions, each bound particle recruits as many receptors as possible (i.e., around κ receptors) and we say we are in the recruiting regime. As z and the number of bound particles increase, more and more receptors are recruited until at some point ($z \sim 10^{-18}$ in the plot) no more receptors are available for further binding. From this point on, further increase in concentration has little effect in the number of bound particles (self-limiting regime). Finally, as z is increases further, the translational entropy cost associated with recruiting receptors becomes larger than the cost of bringing nanoparticles from solution and particles start to "share" receptors, allowing the surface to be fully covered (saturation regime).

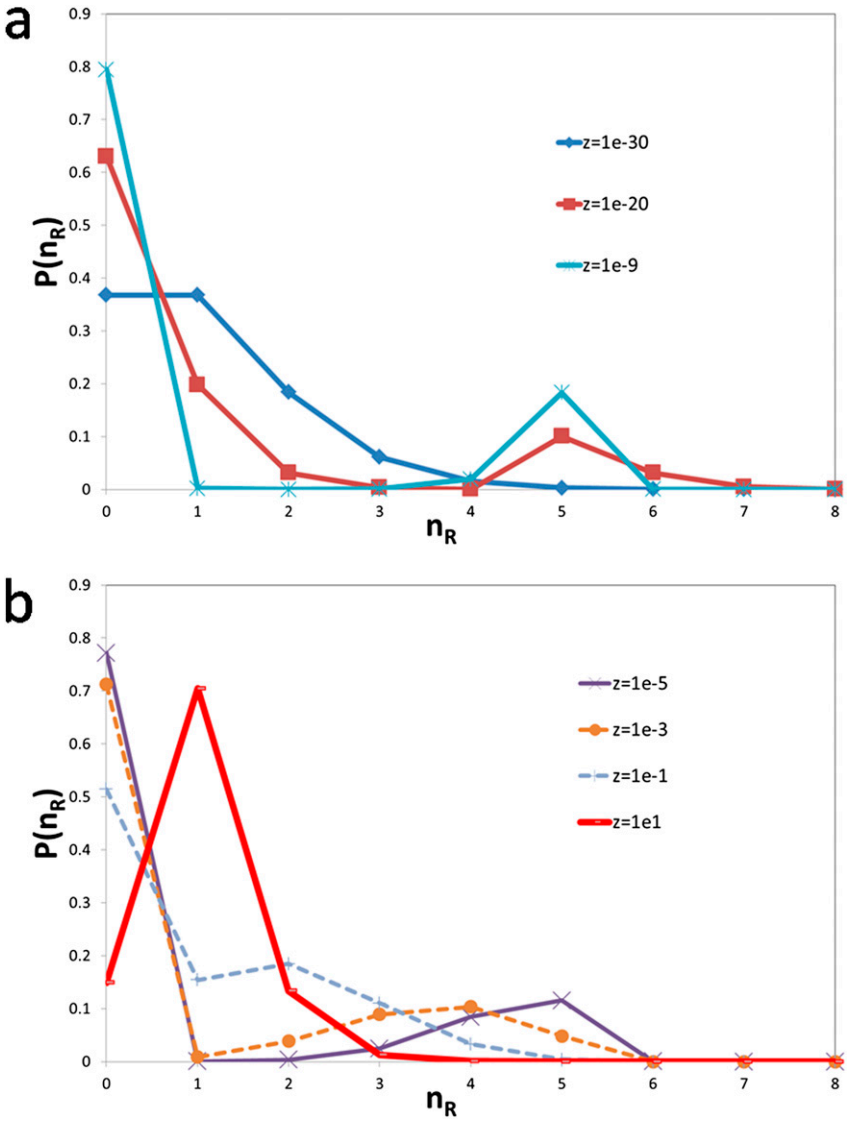

Fig. S9. Probability distributions of finding a lattice site with n_R receptors, for a multivalent system with $<n_R \geq 1$, $\beta f_B = -10$, and $\kappa = 5$ for different values of z. (*A*) For extremely dilute conditions, the receptors distribute randomly (see $z = 10^{-30}$). As the value of z starts to increase, a peak around $n_R = 5$ starts to develop signaling clustering (recruiting regime; see $z = 10^{-20}$) until no receptors are left for further binding (self-limiting regime; see $z = 10^{-9}$). (*B*) When $z^*q(n_R \leq n_R >) \sim 1$, the self-limiting regime ends and further particles start to bind to the surface (saturation regime). In this case, the particles start to "share" receptors and clustering is diminished. As a consequence, the right peak of the bimodal probability distribution starts to shifts to left until it becomes unimodal again with a peak in $n_R \leq n_R >$.